3. Takemoto M, Liao JK. Pleiotropic effects of 3-hydroxy-3-methylglutaryl coenzyme A reductase inhibitors. *Arterioscler Thromb Vasc Biol.* 2001; 21:1712–1719.
4. Egashira K, Hirooka Y, Kai H, Sugimachi M, Suzuki S, Inou T, Takeshita A. Reduction in serum cholesterol with pravastatin improves endothelium-dependent coronary vasomotion in patients with hypercholesterolemia. *Circulation.* 1994;89:2519–2524.
5. Egashira K. Clinical importance of endothelial function in arteriosclerosis and ischemic heart disease. *Circ J.* 2002;66:529–533.
6. Ni W, Egashira K, Kataoka C, Kitamoto S, Koyanagi M, Inoue S, Takeshita A. Anti-inflammatory and antiarteriosclerotic actions of HMG-CoA reductase inhibitors in a rat model of chronic inhibition of nitric oxide synthesis. *Circ Res.* 2001;89:415–421.
7. Girgis RE, Mozammel S, Champion HC, Li D, Peng X, Shimoda L, Tuder RM, Johns RA, Hassoun PM. Regression of chronic hypoxic pulmonary hypertension by simvastatin. *Am J Physiol.* 2007;292: L1105–L1110.
8. Nishimura T, Faul JL, Berry GJ, Vaszar LT, Qiu D, Pearl RG, Kao PN. Simvastatin attenuates smooth muscle neointimal proliferation and pulmonary hypertension in rats. *Am J Respir Crit Care Med.* 2002;166: 1403–1408.
9. Nishimura T, Vaszar LT, Faul JL, Zhao G, Berry GJ, Shi L, Qiu D, Benson G, Pearl RG, Kao PN. Simvastatin rescues rats from fatal pulmonary hypertension by inducing apoptosis of neointimal smooth muscle cells. *Circulation.* 2003;108:1640–1645.
10. McMurtry MS, Bonnet S, Michelakis ED, Bonnet S, Haromy A, Archer SL. Statin therapy, alone or with rapamycin, does not reverse monocrotaline pulmonary arterial hypertension: the rapamycin-atorvastatin-simvastatin study. *Am J Physiol.* 2007;293:L933–L940.
11. Rhodes CJ, Davidson A, Gibbs JS, Wharton J, Wilkins MR. Therapeutic targets in pulmonary arterial hypertension. *Pharmacol Ther.* 2009;121: 69–88.
12. Kimura S, Egashira K, Chen L, Nakano K, Iwata E, Miyagawa M, Tsujimoto H, Hara K, Morishita R, Sueishi K, Tominaga R, Sunagawa K. Nanoparticle-mediated delivery of nuclear factor-κB decoy into lungs ameliorates monocrotaline-induced pulmonary arterial hypertension. *Hypertension.* 2009;53:877–883.
13. Kubo M, Egashira K, Inoue T, Koga J, Oda S, Chen L, Nakano K, Matoba T, Kawashima Y, Hara K, Tsujimoto H, Sueishi K, Tominaga R, Sunagawa K. Therapeutic neovascularization by nanotechnology-mediated cell-selective delivery of pitavastatin into the vascular endothelium. *Arterioscler Thromb Vasc Biol.* 2009;29:796–801.
14. Oda S, Nagahama R, Nakano K, Matoba T, Kubo M, Sunagawa K, Tominaga R, Egashira K. Nanoparticle-mediated endothelial cell-selective delivery of pitavastatin induces functional collateral arteries (therapeutic arteriogenesis) in a rabbit model of chronic hind limb ischemia. *J Vasc Surg.* 2010;52:412–420.
15. Kawashima Y, Yamamoto H, Takeuchi H, Hino T, Niwa T. Properties of a peptide containing DL-lactide/glycolide copolymer nanospheres prepared by novel emulsion solvent diffusion methods. *Eur J Pharm Biopharm.* 1998;45:41–48.
16. Kawashima Y, Yamamoto H, Takeuchi H, Fujioka S, Hino T. Pulmonary delivery of insulin with nebulized DL-lactide/glycolide copolymer (PLGA) nanospheres to prolong hypoglycemic effect. *J Control Release.* 1999;62:279–287.
17. Ikeda Y, Yonemitsu Y, Kataoka C, Kitamoto S, Yamaoka T, Nishida K, Takeshita A, Egashira K, Sueishi K. Anti-monocyte chemoattractant protein-1 gene therapy attenuates pulmonary hypertension in rats. *Am J Physiol Heart Circ Physiol.* 2002;283:H2021–H2028.
18. Urboniene D, Haber I, Fang YH, Thenappan T, Archer SL. Validation of high-resolution echocardiography and magnetic resonance imaging versus high-fidelity catheterization in experimental pulmonary hypertension. *A J Physiol.* 2010;299:401–412.
19. Ohtani K, Egashira K, Nakano K, Zhao G, Funakoshi K, Ihara Y, Kimura S, Tominaga R, Morishita R, Sunagawa K. Stent-based local delivery of nuclear factor-κB decoy attenuates in-stent restenosis in hypercholesterolemic rabbits. *Circulation.* 2006;114:2773–2779.
20. Kojima J, Fujino H, Yosimura M, Morikawa H, Kimata H. Simultaneous determination of NK-104 and its lactone in biological samples by column-switching high-performance liquid chromatography with ultraviolet detection. *J Chromatogr.* 1999;724:173–180.
21. Hampl V, Bibova J, Banasova A, Uhlik J, Mikova D, Hnilickova O, Lachmanova V, Herget J. Pulmonary vascular iNOS induction participates in the onset of chronic hypoxic pulmonary hypertension. *Am J Physiol.* 2006;290:L11–L20.

ONLINE SUPPLEMENT

Nanoparticle-Mediated Delivery of Pitavastatin into Lungs Ameliorates Development and Induces Regression of Monocrotaline-induced Pulmonary Arterial Hypertension

Ling Chen, Kaku Nakano, Satoshi Kimura, Tetsuya Matoba, Eiko Iwata, Miho Miyagawa, Hiroyuki Tsujimoto, Kazuhiro Nagaoka, Junji Kishimoto, Kenji Sunagawa, Kensuke Egashira

Department of Cardiovascular Medicine (LC, KN, TM, EI, MM, KN, KS, KE) and Digital Medicine Initiative (JK), Graduate School of Medical Science, Kyushu University, Fukuoka, Japan; and Hosokawa Micron Corporation (HT), Osaka, Japan.

Address for correspondence:
Kensuke Egashira, M.D. Ph.D.
Department of Cardiovascular Medicine
Graduate School of Medical Science, Kyushu University
3-1-1, Maidashi, Higashi-ku,
Fukuoka 812-8582, Japan
Phone : +81-92-642-5358
Fax : +81-92-642-5375
E-mail: egashira@cardiol.med.kyushu-u.ac.jp

Materials and Methods

Echocardiographic measurements of RV and PA hemodynamics

Transthoracic 2-D, M-mode and pulsed-wave Doppler Echo were obtained with a 30 MHz transducer (Vevo 2100 ultrasound system; Primetech Inc). [1] M-mode and 2-D modalities were applied to measure RV free wall thickness during end diastole and RV wall stress. These images were obtained from the right side of the rat, with the ultrasonic beam positioned perpendicularly to the wall of the midthird of the RV.
PA diameter was measured at the level of pulmonary outflow tract during midsystole using the superior angulation of the parasternal short-axis view. M-mode measurements were performed from "leading edge to leading edge" (epicardial to endocardial) as recommended by the American Society of Echocardiography.
Pulsed-wave Doppler was used to measure PA acceleration time (PAAT) and PA flow velocity time integral. The Doppler sample volume was centrally positioned within the main PA, just distal from the pulmonary valve with the beam oriented parallel to the flow. The sweep speed for the Doppler flow recordings was 400–800 mm/s. RV ejection time was measured as the interval from the onset to the end of ejection in milliseconds. Thereafter, pulmonary artery acceleration time normalized for cycle length, RV systolic pressure, and pulmonary vascular resistance (PVR) were estimated. Stroke volume (SV), CO, and cardiac index (CI) were also calculated.

Measurement of lactate dehydrogenase To examine cytotoxicity of intratracheal treatment of pitavastatin-NP, the activity of lactate dehydrogenase (LDH) in bronchoalveolar lavage fluid (BALF) and lung tissue homogenates was measured 7 days after MCT administration using an assay kit LDH (Wako Pure Chemical Industries, Ltd.) according to the manufacturer's instructions in separate series of experiments.

Measurement of biomarkers by multiplex immunoassay Tissue concentrations of various biomarkers in ling tissue homogenates were measured 7 days after MCT administration using the Luminex LabMAP instruments (Table III), which was ordered to biomarker analysis services of Charles River Inc (http://www.criver.com/en-US/ProdServ/ByType/Discovery/Pages/PlasmaBiomarkerAnalysis.aspx).

1. Urboniene D, Haber I, Fang YH, Thenappan T, Archer SL. Validation of High-Resolution Echocardiography and Magnetic Resonance Imaging Versus High-Fidelity Catheterization in Experimental Pulmonary Hypertension. *Am J Physiol Lung Cell Mol Physiol.*

Table S1. Echocardiographic characteristics of untreated control and MCT-induced PAH rats in prevention study

parameters	untreated control	MCT-induced PAH			
		PBS	FITC NP	Pitava alone	Pitava-NP
Cardiac output (mL/min)	120 ± 17	97 ±21	104 ±20	102 ±20	113 ±16
Stroke volume (mL)	0.29±0.04	0.24±0.05	0.26±0.06	0.26±0.05	0.28±0.05
Heart rate (beats per minute)	412 ± 26	408 ±36	399 ±39	397 ±32	405 ±25
PAAT/cl (x 100)	18 ±1	7 ±1*	7 ±1*	7 ±1*	12 ±1*†
eRVSP (mmHg)	20 ±3	65 ±11*	66 ±9*	62 ±7*	41 ±5 *†
PVR (mmHg/ml/min)	0.12 ±0.02	0.46 ±0.20*	0.43 ±0.12*	0.40 ±0.01*	0.24 ±0.05*†
RV wall thickness (mm)	0.64 ±0.05*	1.16 ±0.14*	1.05 ±0.10*	0.97 ± 0.06*	0.88 ±0.09*†
RV wall stress	20 ±5	48 ±19*	56 ± 26*	48 ±12*	24 ±8†

Data are the mean± SEM (n=6 each).
*P< 0.05 versus untreated control group
† P< 0.05 versus PBS group.
Abbreviations: PAAT/cl = normalized pulmonary artery acceleration time; eRVSP = estimated RV systolic pressure; PVR = pulmonary vascular resistance.

Table S2. Lactate dehydrogenase activity in cell-free bronchial lavage fluid and lung tissue homogenates 7 days after monocrotaline administration

		monocrotaline			
Sample sites	Untreated control	PBS group	FITC NP group	Pitava alone group	Pitava NP group
bronchial lavage fluid (IU/mL)	ND	ND	ND	ND	ND
Lung tissue (IU/ng protein)	8.6±3.4	2.8±1.1	10.9±6.0	5.7±4.6	11.8±4.9

Data are the mean± SEM (n=6 each). ND = not detected (under limit of detection).
There is no significant difference (P=0.56) among 5 groups by one-way ANOVA.

Table S3. Cytokines and other proteins in lung tissue homogenates 7 days after monocrotaline administration

parameters	unit	Untreated control	PBS group	FITC NP group	Pitava alone group	Pitava NP group
Apo A1	μg/mg	0.14±0.05	0.10±0.03	0.09±0.01	0.10±0.01	0.10±0.01
CD40	pg/mg	N.D.	N.D.	N.D.	N.D.	N.D.
CD40 Ligand	pg/mg	43±16	34±14	25±3	30±8	39±13
CRP	μg/mg	1.3±0.3	1.2±0.2	1.3±0.4	1.3±0.2	1.6±0.2
ET-1	pg/mg	61±36	67±29	61±18	64±15	56±15
Eotaxin	pg/mg	49±12	53±15	40±8	45±17	63±11
EGF mouse	pg/mg	0.54±0.21	0.55±0.21	0.40±0.08	0.44±0.09	0.44±0.07
Factor VII	ng/mg	0.53±0.12	0.58±0.17	0.47±0.07	0.48±0.07	0.53±0.08
FGF-9	ng/mg	0.10±0.02	0.09±0.03	0.07±0.01	0.08±0.01	0.08±0.03
FGF-basic	ng/mg	0.21±0.04	0.21±0.06	0.17±0.04	0.22±0.04	0.24±0.04
GCP-2 Rat	pg/mg	6.5±1.6	7.4±3.2	6.7±1.3	8.1±1.0	7.6±7
GM-CSF	pg/mg	N.D.	N.D.	N.D.	N.D.	N.D.
Haptoglobin	μg/mg	0.80±0.30	1.13±0.40	1.04±0.26	1.19±0.12	1.18±0.25
IFN-gamma	pg/mg	0.12±0.06	0.24±0.09	0.23±0.10	0.18±0.07	0.18±0.05
IP-10	pg/mg	1.7±0.3	2.2±1.0	1.7±0.3	1.7±0.5	2.1±0.8
IL-1 alpha	pg/mg	5.3±4.8	9.7±7.1	4.6±1.0	7.8±2.9	5.7±3.3
IL-1 beta	ng/mg	N.D.	N.D.	N.D.	N.D.	N.D.
IL-10	pg/mg	3.1±1.5	2.5±1.5	1.4±0.8	1.8±0.3	1.9±0.9
IL-11	pg/mg	9.8±5.6	6.1±1.6	6..1±4.8	5.9±1.0	6.8±2.0
IL-12p70	pg/mg	1.5±0.4	1.3±0.4	1.2±0.4	1.0±0.1	1.2±0.4
IL-17A	pg/mg	0.2±0.04	0.2±0.09	0.2±0.05	0.2±0.05	0.2±0.02
IL-18	ng/mg	0.2±0.1	0.2±0.1	0.2±0.1	0.2±0.0	0.2±0.1
IL-2	pg/mg	1.7±0.7	1.4±1.1	0.6±0.3	0.8±0.6	0.9±0.7
IL-3	pg/mg	1.1±0.5	0.9±0.3	0.9±0.4	0.7±0.3	0.8±0.2
IL-4	pg/mg	N.D.	N.D.	N.D.	N.D.	N.D.
IL-5	ng/mg	N.D.	N.D.	N.D.	N.D.	N.D.
IL-6	pg/mg	N.D.	N.D.	N.D.	N.D.	N.D.
IL-7	pg/mg	3.9±0.7	3.5±2.0	3.4±0.8	3.0±0.3	3.2±0.6
LIF	pg/mg	33.9±9.8	38.3±12.5	29.9±4.3	31.6±4.1	35.7±6.1
Lymphotactin	pg/mg	1.7±0.4	2.0±0.7	1.8±0.3	1.6±0.1	1.78±0.4
MIP-1alpha	ng/mg	0.05±0.02	0.06±0.02	0.05±0.01	0.05±0.00	0.05±0.01
MIP-1beta	pg/mg	26.7±7.6	36.8±13.2	30.9±13.2	27.1±5.2	28.2±5.8
MIP-2	pg/mg	1.7±1.0	1.3±0.3	1.5±0.5	1.8±0.9	1.8±0.5
MIP-3 beta	ng/mg	0.1±0.0	0.2±0.1	0.1±0.0	0.2±0.0	0.2±0.0
MDC	pg/mg	14±5	11±3	12±1	15±5	15±3
MMP-9	pg/mg	16±3	13±6	13±3	14±3	13±3
MCP-1	pg/mg	14±2	17±4	17±4	16±4	20±4
MCP-3	pg/mg	12±3	14±4	13±3	13±3	16±4
MPO	ng/mg	26±12	25±14	15±4	15±5	26±6
Myoglobin	ng/mg	109±26	157±130	138±67	135±54	133±69
OSM	pg/mg	9±2	11±3	9±1	9±0.001	10±2
SAP	pg/mg	0.007±0.002	0.007±0.002	0.006±0.001	0.008±0.001	0.008±0.001
SGOT	μg/mg	N.D.	N.D.	N.D.	N.D.	N.D.
SCF	pg/mg	920±509	404±71	421±143	603±440	531±110
RANTES	pg/mg	0.82±0.51	0.55±0.35	0.56±0.50	0.56±0.31	0.56±0.25
TPO	ng/mg	0.41±0.09	0.39±0.15	0.32±0.11	0.23±0.14	0.27±0.08
TF	ng/mg	0.15±0.03	0.15±0.05	0.15±0.03	0.14±0.03	0.14±0.04

TIMP-1	pg/mg	4±8	3.8±1.2	3.6±0.8	3.5±0.5	3.6±0.6
TNF-alpha	ng/mg	2.4±0.5	2.7±0.7	2.3±0.5	2.1±0.2	2.2±0.5
VCAM-1	ng/mg	4.8±1.0	5.4±1.8	5.2±1.0	5.2±0.9	5.8±0.7
VEGF-A	pg/mg	749±297	759±281	924±317	791±181	689±214
vWF	ng/mg	0.6±0.2	0.5±0.2	0.4±0.1	0.5±0.1	0.5±0.1

Data are mean ± SEM (n= 6 each).
Multiplex immunoassay were peformed using the Luminex LabMAP instruments.
Apo A1 (Apolipoprotein A1), CD (cluster of differentiation), CRP (C Reactive Protein), EGF (Epidermal Growth Factor), FGF-9 (Fibroblast Growth Factor-9), FGF-basic (Fibroblast Growth Factor-basic), GCP-2 (Granulocyte Chemotactic Protein-2), GM-CSF (Granulocyte Macrophage-Colony Stimulating Factor), GST-a (Glutathione S-Transferase alpha), IFN-g (Interferon-gamma), IgA (Immunoglobulin A), IL (Interleukin), IP-10 (Inducible Protein-10), LIF (Leukemia Inhibitory Factor), MCP (Monocyte Chemoattractant Protein), MDC (Macrophage-Derived Chemokine), MIP (Macrophage Inflammatory Protein), MMP-9 (Matrix Metalloproteinase-9), MPO (Myeloperoxidase), OSM (Oncostatin M), RANTES (Regulation Upon Activation, Normal T-Cell Expressed and Secreted), SAP (Serum Amyloid P), SCF (Stem Cell Factor), SGOT (Serum Glutamic-Oxaloacetic Transaminase), TIMP-1 (Tissue Inhibitor of Metalloproteinase Type-1), TNF-a (Tumor Necrosis Factor-alpha), TPO (Thrombopoietin), VCAM-1 (Vascular Cell Adhesion Molecule-1), VEGF (Vascular Endothelial Cell Growth Factor), vWF (von Willebrand Factor). N.D. (Not Detected).

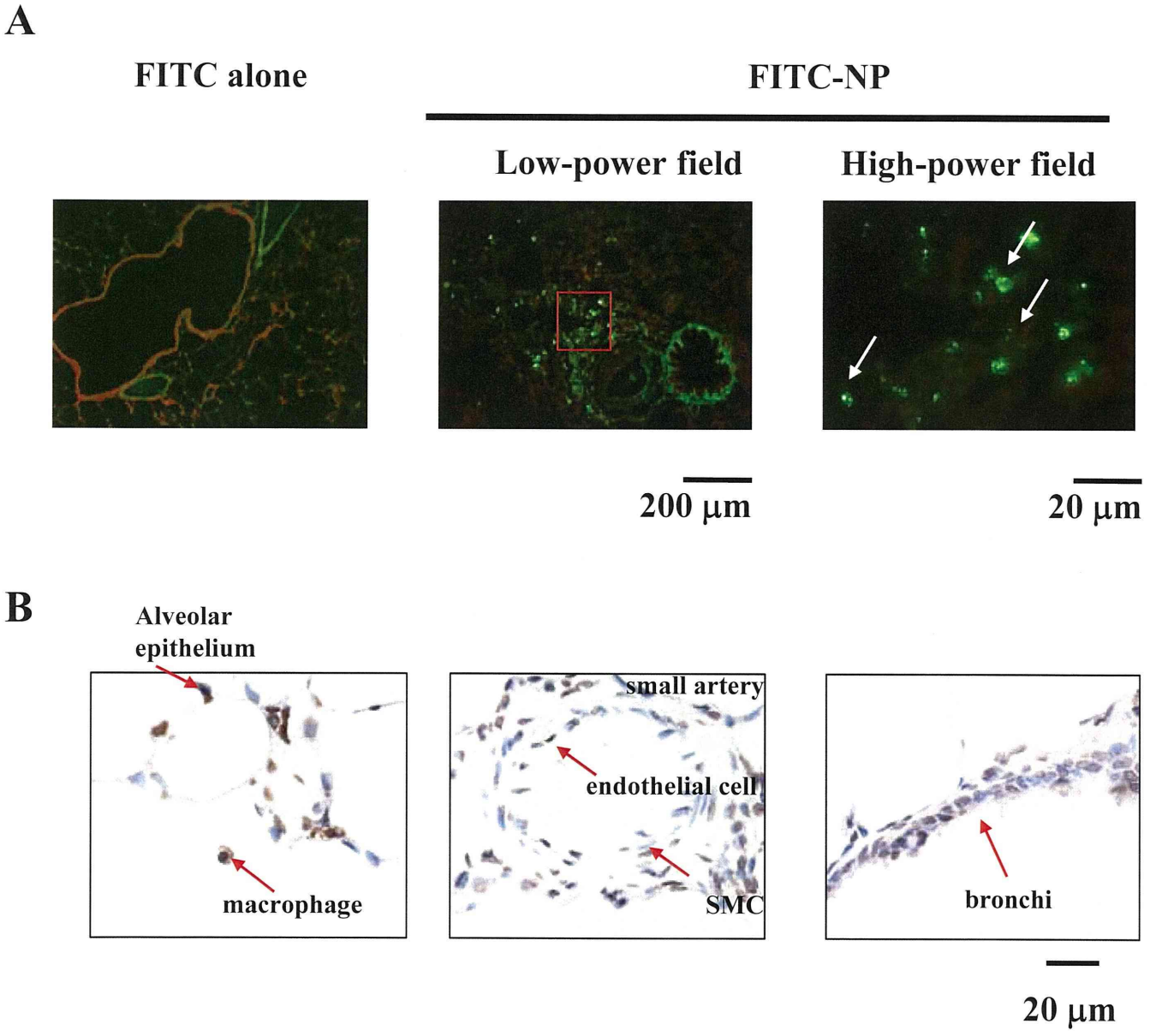

Figure S1. Localization of FITC alone and FITC-NP post-instillation in the rat lung. A, Fluorescent micrographs of cross-sections from lung instillated with FITC alone and FITC-labeled NP on day 3 post-instillation. Nuclei were counterstained with propidium iodide (red). Scale bars: 200 μm and 20 μm.
B, Micrographs of cross-sections stained immunohistochemically against FITC from lung instillated intratracheally with FITC-NP on days 14 post-instillation.

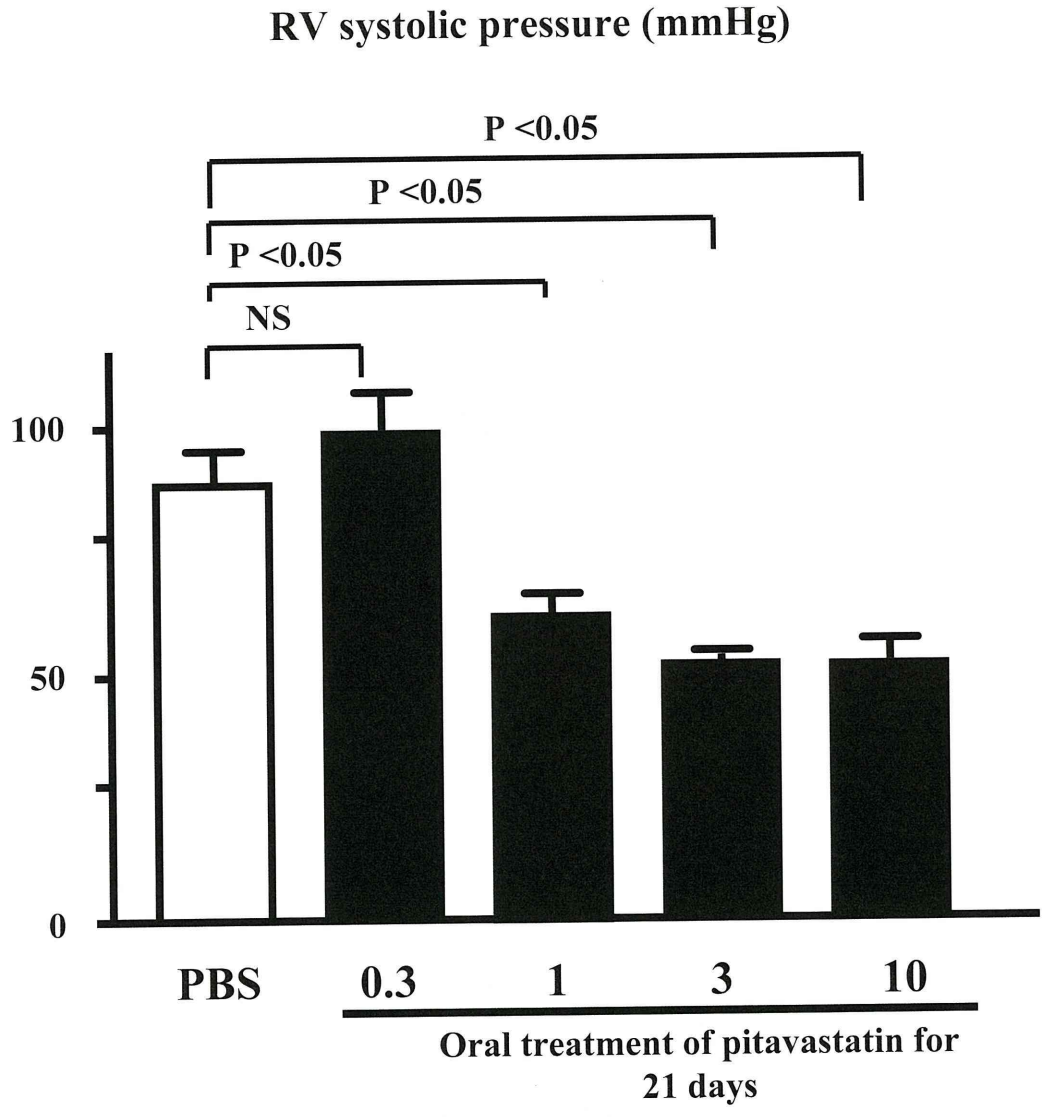

Figure S2. Effects of oral treatment of pitavastatin on right ventricular (RV) systolic pressure 3 weeks after MCT injection. Data are mean ± SEM ($n = 6$ each).

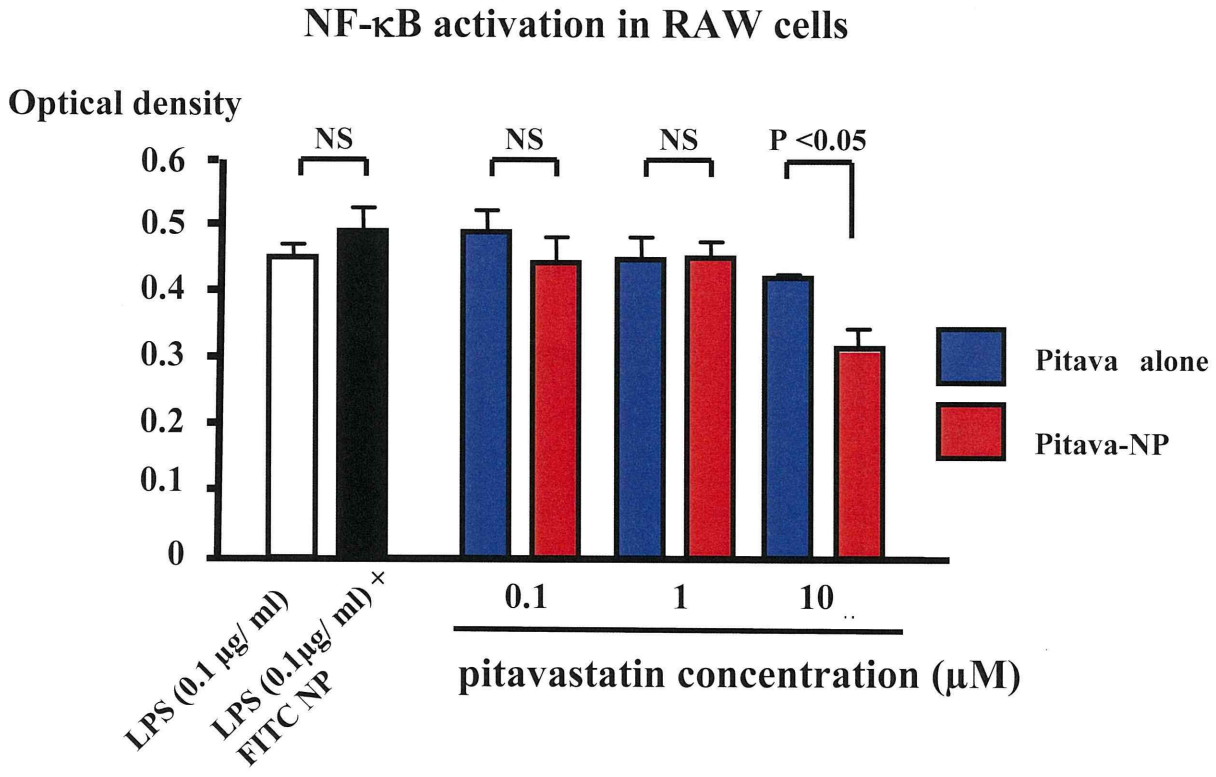

Figure S3 Effect of pitavastatin-NP on NF-κB activation of monocyte cell line (RAW cells)
Effects of pitavastatin-NP on LPS-stimulated activation of NF–κB (ELISA-based DNA binding assay against NF-kB p65 subunit: arbitrary unit). Data are mean ± SEM (n= 6 each).

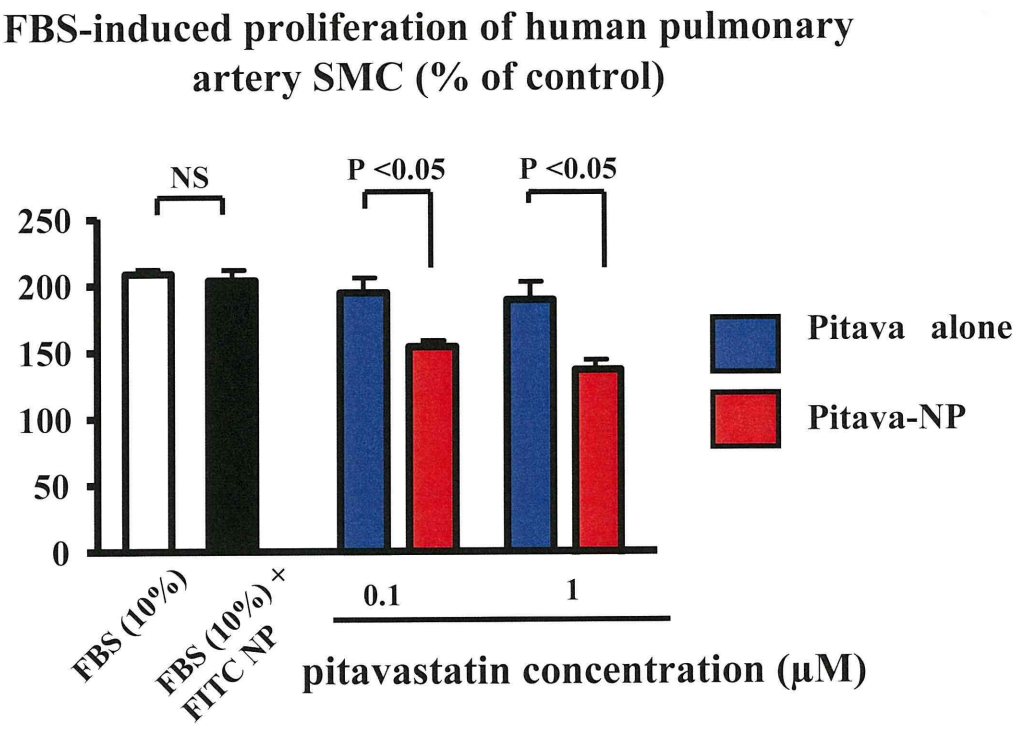

Figure S4. Effects of pitavastatin-NP versus pitavastatin on FBS-induced proliferation of human PASMCs (cell count per well). Data are mean ± SEM (n = 6 each).

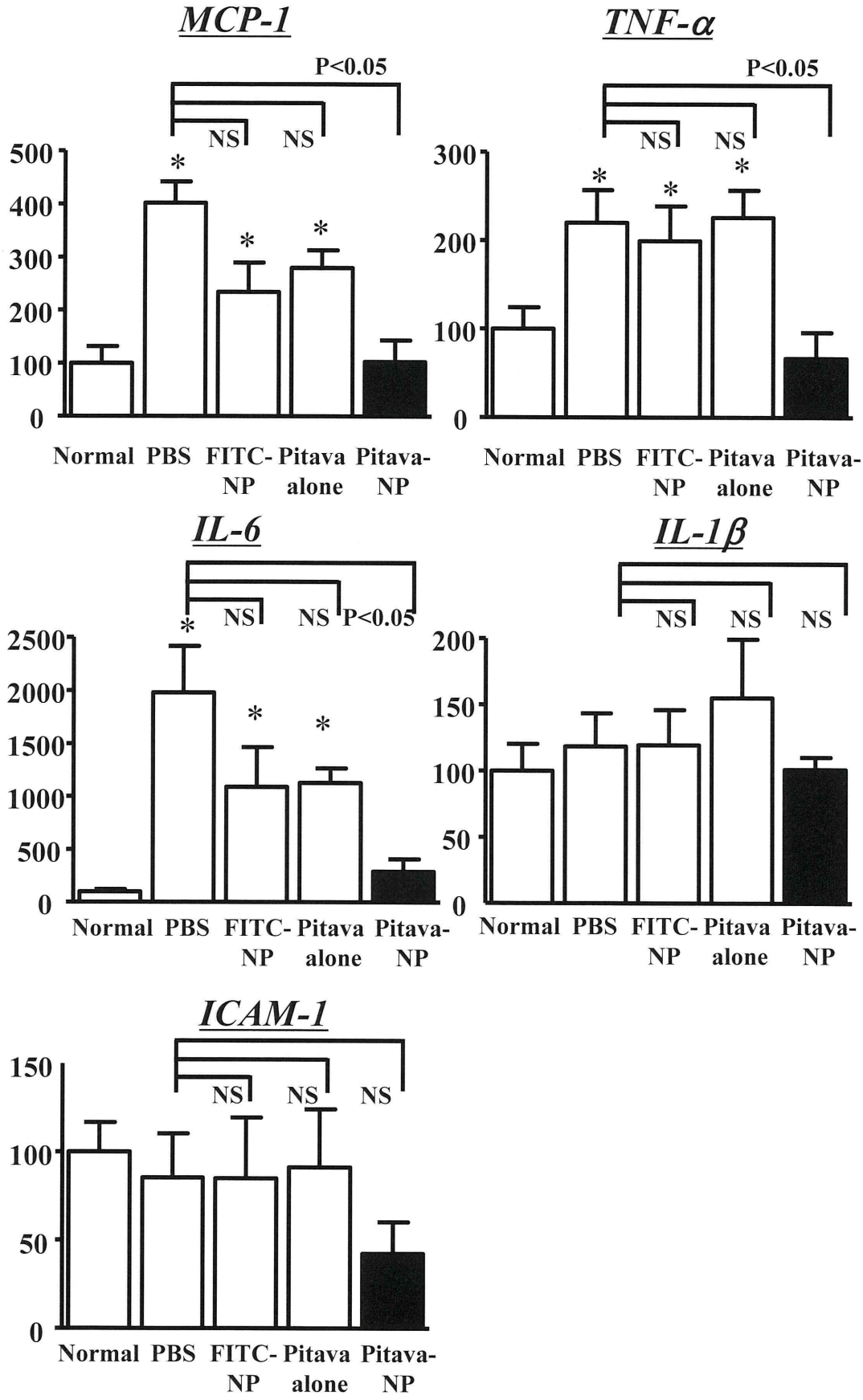

Figure S5. Effects of pitavastatin-NP on mRNA levels of various inflammatory and proliferative factors 21 days after MCT injection (n = 6 each). *$P < 0.05$ versus Normal. Data are mean ± SEM. NS; Not Significant.

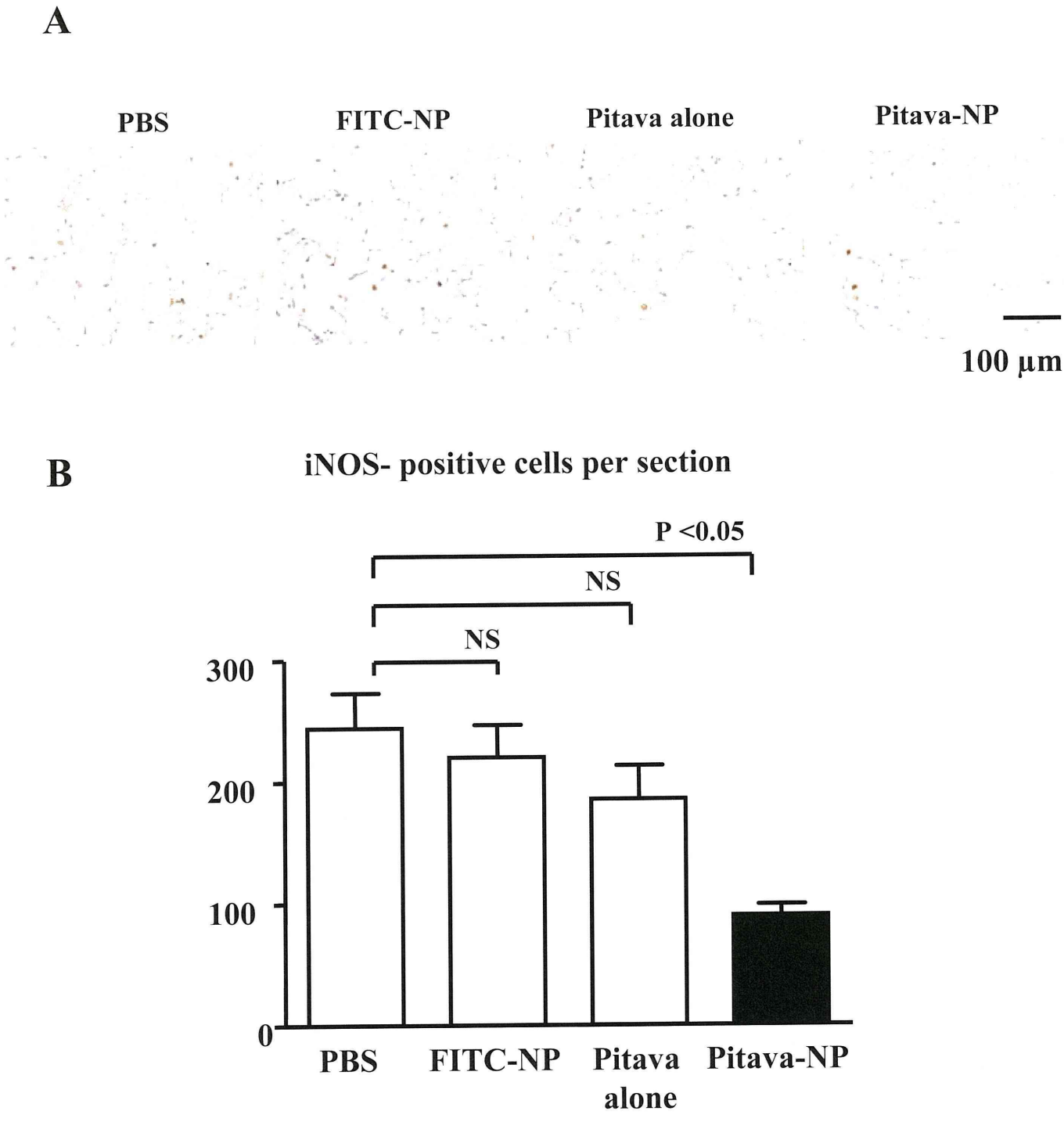

Figure S6. Effects of pitavastatin-NP on iNOS protein expression
A, Representative micrographs of lung tissues stained immunohistochemically for iNOS.
B, Effects of pitavastatin-NP on infiltration of iNOS-positive cells 21 days after MCT injection. Data are mean ±SEM (n = 6 each).

INTERNAL MEDICINE

□ CASE REPORT □

A Case of Multiple Focal Nodular Hyperplasia in the Liver Which Developed after Heart Transplantation

Takeo Fujino, Mari Nishizaka, Takeo Yufu and Kenji Sunagawa

Abstract

An 18-year-old woman, who had undergone cardiac allograft transplantation, developed continuous back pain two months after surgery. Abdominal computed tomography showed multiple enhanced lesions in her liver, which were not present before transplantation. One tumor bulged from the surface of the liver and compressed the stomach. Partial resection of the liver was performed and her symptoms improved. The pathological diagnosis was focal nodular hyperplasia (FNH). To our knowledge, this is the first report of multiple FNH after heart transplantation. Transplant clinicians may need to keep this possibility under consideration following heart transplantation.

Key words: heart transplantation, complications, multiple focal nodular hyperplasia

(Intern Med 50: 43-46, 2011)
(DOI: 10.2169/internalmedicine.50.4282)

Introduction

Focal nodular hyperplasia (FNH) is a benign liver tumor, which is often seen in young women. However, multiple FNH is rare. The pathogenesis of FNH is not well understood. There are many possible complications we should be aware of following heart transplantation. Here we present the first case, to our knowledge, of development of multiple FNH after heart transplantation. The current case is instructive and indicates that we should keep this possibility under consideration if new liver lesions were detected after heart transplantation.

Case Report

An 18-year-old female cardiac allograft recipient was referred to our hospital for suspected rejection six months after transplant. She underwent transplantation in January 2008 for uncontrollable right ventricular (functional left ventricular) dysfunction due to corrected transposition of the great arteries, status post Rastelli operation, tricuspid valve replacement, and cardiac resynchronization therapy (CRT). She had been taking oral contraceptives for about two years since menarche until heart transplantation to prevent anemia that could worsen heart failure. After the transplantation surgery, she started taking oral immunosuppressant agents including prednisolone 10 mg per day, mycophenolate mofetil 500 mg per day, and cyclosporine A, the trough concentration of which was regularly monitored to be maintained in the range of 160-240 ng/mL.

In March 2008 she developed continuous back pain. Osteoporotic bone disease was excluded. Steroid pulse therapy was given on suspicion of acute rejection, but her symptom did not improve. Therefore, in July, she was referred to our hospital for further investigation.

Physical examination did not show any abnormal findings, such as eczema, rush or abdominal pain. Her blood tests, chest X-ray, electrocardiogram, and cardiac echocardiography did not suggest the cause of her symptom. Cardiac catheterization revealed almost normal hemodynamics. Her coronary arteries were intact without any vasculopathy on coronary angiography and intravascular ultrasonography. Endomyocardial biopsy did not explain her symptom either with the tissue showing minimum cellular rejection Grade 1 R by Standardized Cardiac Biopsy Grading (1).

During her evaluation, abdominal computed tomography (CT) showed multiple enhanced lesions in the liver, which had not been seen prior to heart transplantation in March 2004 (Fig. 1A, 1B). Central scars were not apparent in the

Department of Cardiovascular Medicine, Kyushu University Hospital, Japan
Received for publication July 28, 2010; Accepted for publication September 17, 2010
Correspondence to Dr. Takeo Fujino, tafujino@cardiol.med.kyushu-u.ac.jp

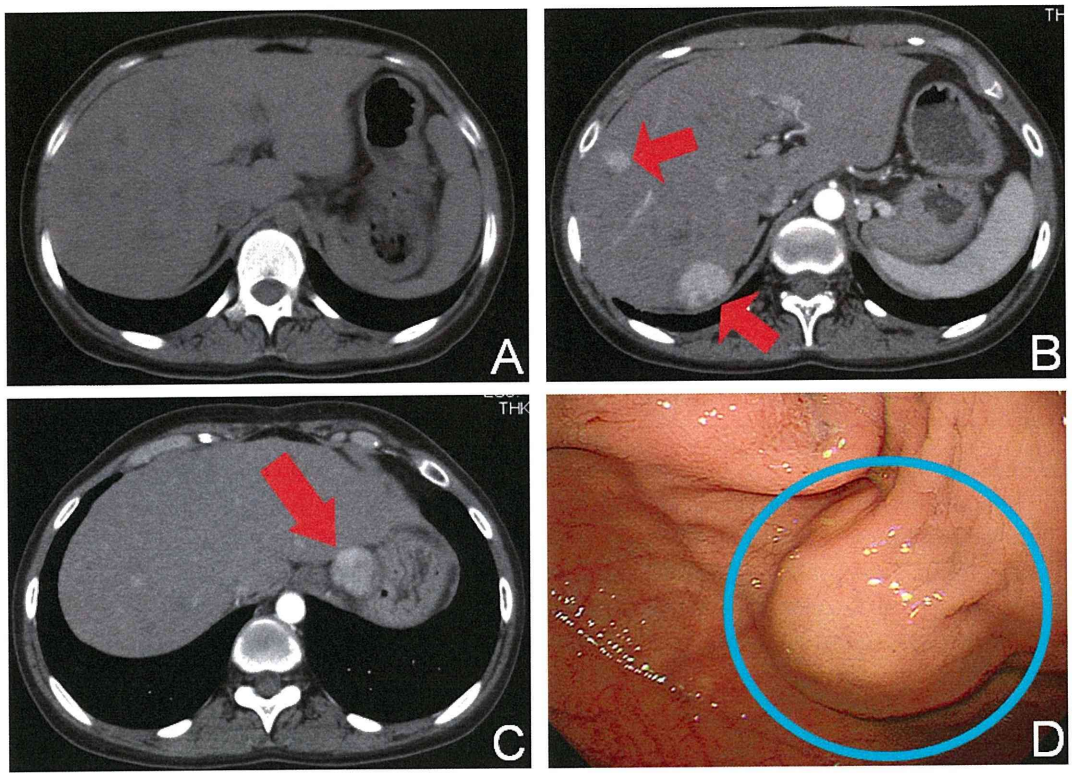

Figure 1. **A: Computed tomography of the liver did not show any distinct lesions four years before heart transplantation. B: Computed tomography showed multiple lesions (arrows) seven months after heart transplantation. C: Computed tomography showed a distinct tumor in the left lateral segment of the liver (arrow). D: Endoscopic findings of the stomach; the tumor bulged from the surface of the liver and compressed the stomach (circle).**

lesions. We considered magnetic resonance imaging (MRI), which is considered to be more informative for the differential diagnosis of liver tumors (2). However, as the leads of CRT-defibrillator (CRT-D) were still in her vein, MRI was not possible.

One tumor in the left lateral segment bulged from the surface of the liver and compressed the stomach (Fig. 1C, 1D). Since it was suspected to be related to her back pain and because there was fear of rupture and possible malignancy (including posttransplant lymphoproliferative disease), partial resection of the liver was performed in October 2008 (Fig. 2A, 2B). The pathological findings of the tumor included hyperplastic hepatocytes with acinar structure, ductular reaction, abnormal vessels, and central scar (Fig. 2C-F), which are typical findings of FNH. Her back discomfort improved after the surgery. In fact, even though the residual lesions are slowly enlarging, back pain remains absent about two years after surgery.

Discussion

There are many possible complications after heart transplantation, such as rejection, coronary vasculopathy, infection, and malignancy (3). We can never be too careful to notice any unusual symptoms or signs in transplant recipients, as they are often atypical presentations of these pathological complications. The present patient complained of continuous back pain. We considered the above possibilities and attempted to determine the cause of her complaint. In the process of her evaluation, many nodular lesions were detected in her liver, which had not been present before heart transplantation. The pathological diagnosis of the tumors was found to be FNH. After surgical resection, her back pain resolved. We presume, in the current case, FNH was related to her complaint.

FNH is one of the most common benign neoplasms of the liver, which accounts for 8% of all primary hepatic tumors. It is more commonly found in women (4). In most cases it appears solitary. Multiple FNH is extremely rare, and few reports exist in the literature (5). The pathogenesis of multiple FNH is not well understood. In the current case, the etiology of the multiple FNH cannot be definitively attributed to her prior heart transplantation. Other possible contributing factors present before and after transplantation, including the use of oral contraceptives, surgical stress, and immunosuppressant therapy.

A possible relation between FNH and oral contraceptive use has been proposed but remains controversial (6). In the current case, the recipient had been taking oral contraceptives for about two years since menarche preceding heart transplantation to prevent anemia, which may have contributed to the development of multiple FNH. Because candi-

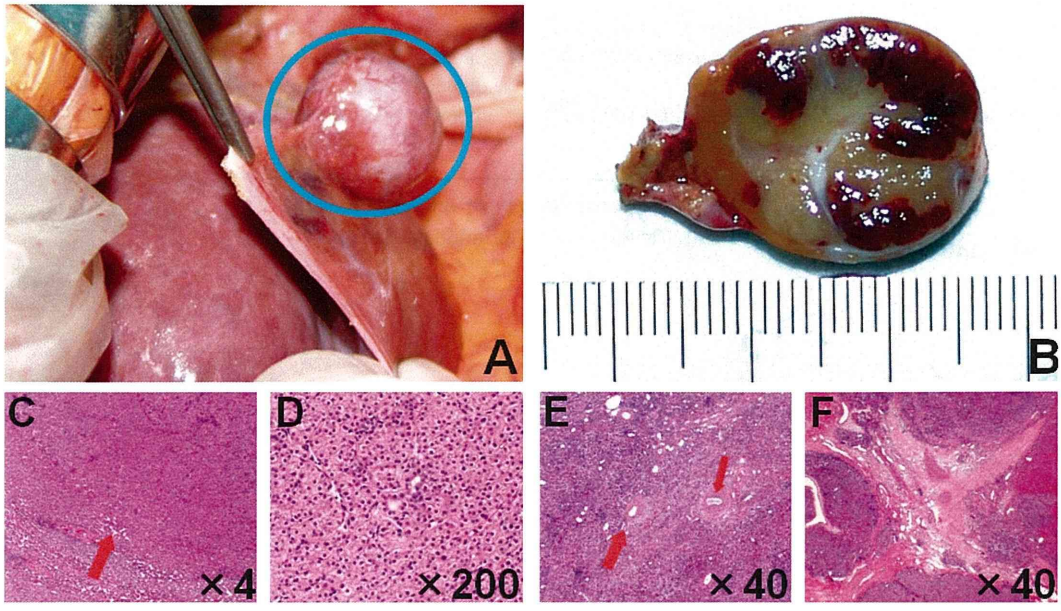

Figure 2. **Intraoperative findings of the tumor. A: A distinct tumor in the left lateral segment bulged from the surface of the liver (circle). It was round with a smooth surface, and the texture was elastic and hard. B: The surface of the tumor was encased by a membranous layer, and the section of the tumor showed well-demarcated lesions inside. The tumor was 2.5×2.5 cm in size. C-F: Microscopic sections of the tumor (Hematoxylin and Eosin staining). C and D show hyperplastic hepatocytes (arrows). E shows abnormal vessels (arrows). F shows central scar of the tumor. They are typical findings of focal nodular hyperplasia.**

dates for heart transplantation suffer from severe heart failure, it is not unusual to receive oral contraceptives to prevent anemia or pregnancy. The current report suggests that development of FNH should be especially considered in such patients.

There is no evidence for the relationship between immunosuppressants and FNH, but immunosuppressant agents are causally related to malignant tumors, including post-transplant lymphoproliferative disease (7). The current patient needs to continue immunosuppressant therapy. With no evidence for rejection having been seen during periodic cardiac biopsy, we have been modulating her agents carefully. In fact, the residual lesions are slowly enlarging after surgery, but surgical resection of the liver for treatment of FNH is not indicated unless the patient has symptoms related to the tumor size or location (4). Our clinical plan includes periodic abdominal CT in order to monitor the residual tumors.

In this case we diagnosed FNH by tissue pathology, but, in general, diagnosis by imaging is preferred. For non-invasive diagnosis, MRI is more useful than CT, the sensitivity and specificity of which are 70% and 98%, respectively (2). The patient, however, could not undergo MRI because CRT-D leads were still in her vein. In addition, because one tumor was suspected of causing her back pain and because of risk of rupture, we chose prompt surgical resection.

Again, the causality cannot be proven. However, this is an instructive case; the first case report, to our knowledge, of multiple FNH observed after heart transplantation, although FNH is not rare after hematopoietic stem cell transplantation (8). To the best of our knowledge, there are no case reports of FNH after solid organ transplantation. Data of Japanese patients after heart transplantation are scarce, and accumulation of such data will be clinically useful. Based on the present report, we suggest that multiple FNH should be considered if new liver lesions are detected after heart transplantation, especially if the patient had taken oral contraceptives before surgery.

The authors state that they have no Conflict of Interest (COI).

References

1. Stewart S, Winters GL, Fishbein MC, et al. Revision of the 1990 working formulation for the standardization of nomenclature in the diagnosis of heart rejection. J Heart Lung Transplant **24**: 1710-1720, 2005.
2. Vilgrain V. Focal nodular hyperplasia. Eur J Radiol **58**: 236-245, 2006.
3. Tjang YS, van der Heijden GJ, Tenderich G, Grobbee DE, Korfer R. Survival analysis in heart transplantation: results from an analysis of 1290 cases in a single center. Eur J Cardiothorac Surg **33**: 856-861, 2008.
4. Bonney GK, Gomez D, Al-Mukhtar A, Toogood GJ, Lodge PA, Prasad R. Indication for treatment and long-term outcome of focal nodular hyperplasia. HPB (Oxford) **9**: 368-372, 2007.
5. Kim J, Nikiforov YE, Moulton JS, Lowy AM. Multiple focal nodular hyperplasia of the liver in a 21-year-old woman. J Gastrointest Surg **8**: 591-595, 2004.

6. Giannitrapani L, Soresi M, La Spada E, Cervello M, D'Alessandro N, Montalto G. Sex hormones and risk of liver tumor. Ann N Y Acad Sci **1089**: 228-236, 2006.
7. Zafar SY, Howell DN, Gockerman JP. Malignancy after solid organ transplantation: an overview. Oncologist **13**: 769-778, 2008.
8. Suduour H, Mainard L, Baumann C, Clement L, Salmon A, Bordigoni P. Focal nodular hyperplasia of the liver following hematopoietic SCT. Bone Marrow Transplant **43**: 127-132, 2009.

Circulation Journal
Official Journal of the Japanese Circulation Society
http://www.j-circ.or.jp

ORIGINAL ARTICLE
Hypertension and Circulatory Control

Medetomidine, an α_2-Adrenergic Agonist, Activates Cardiac Vagal Nerve Through Modulation of Baroreflex Control

Shuji Shimizu, MD, PhD; Tsuyoshi Akiyama, MD, PhD; Toru Kawada, MD, PhD; Yusuke Sata, MD; Masaki Mizuno, PhD; Atsunori Kamiya, MD, PhD; Toshiaki Shishido, MD, PhD; Masashi Inagaki, MD; Mikiyasu Shirai, MD, PhD; Shunji Sano, MD, PhD; Masaru Sugimachi, MD, PhD

Background: Although α_2-adrenergic agonists have been reported to induce a vagal-dominant condition through suppression of sympathetic nerve activity, there is little direct evidence that they directly increase cardiac vagal nerve activity. Using a cardiac microdialysis technique, we investigated the effects of medetomidine, an α_2-adrenergic agonist, on norepinephrine (NE) and acetylcholine (ACh) release from cardiac nerve endings.

Methods and Results: A microdialysis probe was implanted into the right atrial wall near the sinoatrial node in anesthetized rabbits and perfused with Ringer's solution containing eserine. Dialysate NE and ACh concentrations were measured using high-performance liquid chromatography. Both 10 and 100 μg/kg of intravenous medetomidine significantly decreased mean blood pressure (BP) and the dialysate NE concentration, but only 100 μg/kg of medetomidine enhanced ACh release. Combined administration of medetomidine and phenylephrine maintained mean BP at baseline level, and augmented the medetomidine-induced ACh release. When we varied the mean BP using intravenous administration of phenylephrine, treatment with medetomidine significantly steepened the slope of the regression line between mean BP and log ACh concentration.

Conclusions: Medetomidine increased ACh release from cardiac vagal nerve endings and augmented baroreflex control of vagal nerve activity. (*Circ J* 2012; **76:** 152–159)

Key Words: Acetylcholine; Norepinephrine; Sinoatrial node; Sympathetic nervous system; Vagus nerve

The selective α_2-adrenergic agonist, dexmedetomidine, is widely used for sedation in intensive care units because it has a less respiratory depressive effect.[1] In addition, several benefits of dexmedetomidine that favor its use in intensive care have been reported, such as reduced opioid dosage requirement. In animal studies, Hayashi et al reported that dexmedetomidine prevented epinephrine-induced arrhythmias in halothane-anesthetized dogs.[2] This antiarrhythmic effect of α_2-adrenergic agonists may be partly ascribed to vagal activation.[3] It has already been reported that central sympathetic inhibition by an α_2-adrenergic agonist, guanfacine, augmented the sleep-related ultradian rhythm of parasympathetic tone in patients with chronic heart failure.[4] Although α_2-adrenergic agonists are widely recognized as inducing a vagal-dominant condition through the suppression of sympathetic nerve, there is little direct evidence that they directly increase cardiac vagal nerve activity, because such activity has been assessed only by indirect methods, such as heart rate variability, in most studies.[5]

Vanoli et al[6] reported that vagal stimulation after an acute ischemic episode effectively prevented ventricular fibrillation in dogs. Their group also indicated that the dogs that developed ventricular fibrillation during the acute ischemic episode had a significantly lower baroreflex-mediated heart rate response,[7] suggesting the importance of the baroreflex in controlling vagal function. If an α_2-adrenergic agonist is able to activate the cardiac vagal nerve directly or via modulation of the baroreflex function, it will provide a new therapeutic option for life-threatening arrhythmias after myocardial ischemia.

Medetomidine is a racemic mixture of 2 stereoisomers, dexmedetomidine and levomedetomidine. However, because it has already been reported that levomedetomidine has no effect on cardiovascular parameters and causes no apparent sedation or analgesia,[8] the pharmacokinetics of dexmedetomidine and racemic medetomidine are almost similar. We hypothesized that medetomidine can activate the cardiac vagal nerve

Received June 1, 2011; revised manuscript received September 6, 2011; accepted September 14, 2011; released online October 29, 2011
Time for primary review: 25 days

Department of Cardiovascular Dynamics (S. Shimizu, T.K., Y.S., M.M., A.K., T.S., M.I., M. Sugimachi), Department of Cardiac Physiology (T.A., M. Shirai), National Cerebral and Cardiovascular Center Research Institute, Suita; and Department of Cardiovascular Surgery, Okayama University Graduate School of Medicine, Dentistry and Pharmaceutical Sciences, Okayama (S. Sano), Japan

Mailing address: Shuji Shimizu, MD, PhD, Department of Cardiovascular Dynamics, National Cerebral and Cardiovascular Center Research Institute, 5-7-1 Fujishiro-dai, Suita 565-8565, Japan. E-mail: shujismz@ri.ncvc.go.jp

ISSN-1346-9843 doi:10.1253/circj.CJ-11-0574

through a central action and improve the baroreflex control of vagal nerve activity. We have established a cardiac microdialysis technique for separate monitoring of neuronal norepinephrine (NE) and acetylcholine (ACh) release to the rabbit sinoatrial (SA) node in vivo.[9–11] Using this microdialysis technique, we investigated the effects of medetomidine on cardiac autonomic nerve activities innervating the SA node.

Methods

Surgical Preparation

Animal care was provided in accordance with the "Guiding principles for the care and use of animals in the field of physiological sciences" published by the Physiological Society of Japan. All protocols were approved by the Animal Subject Committee of the National Cerebral and Cardiovascular Center.

In this study, 31 Japanese white rabbits weighing 2.3–3.0 kg were used. Anesthesia was initiated by an intravenous injection of pentobarbital sodium (50 mg/kg) via the marginal ear vein, and then maintained at an appropriate level by continuous intravenous infusion of α-chloralose and urethane (16 mg·kg^{-1}·h^{-1} and 100 mg·kg^{-1}·h^{-1}) through a catheter inserted into the femoral vein. The animals were intubated and ventilated mechanically with room air mixed with oxygen. Respiratory rate and tidal volume were set at 30 cycles/min and 15 ml/kg, respectively. Systemic arterial pressure was monitored by a catheter inserted into the femoral artery. Esophageal temperature, which was measured by a thermometer (CTM-303, Terumo, Japan), was maintained between 38°C and 39°C using a heating pad.

With the animal in lateral position, a right lateral thoracotomy was performed and the right 3rd to 5th ribs were partially resected to expose the heart. After incising the pericardium, a dialysis probe was implanted as described below. Three stainless steel electrodes were attached around the thoracotomy incision for recording body surface electrocardiogram (ECG). The heart rate was determined from the ECG using a cardiotachometer. Heparin sodium (100 IU/kg) was administered intravenously to prevent blood coagulation. At the end of the experiment, the animal was killed humanely by injecting an overdose of pentobarbital sodium. In the postmortem examination, the right atrial wall was resected en bloc with the dialysis probe. The inside of the atrial wall was observed macroscopically to confirm that the dialysis membrane was not exposed to the right atrial lumen.

Dialysis Technique

The materials and properties of the dialysis probe have been described previously.[9–12] A dialysis fiber of semipermeable membrane (length 4 mm, outer diameter 310 μm, inner diameter 200 μm, PAN-1200, molecular weight cutoff 50,000; Asahi Chemical, Tokyo, Japan) was attached at both ends to polyethylene tubes (length 25 cm, outer diameter 500 μm, inner diameter 200 μm). A fine guiding needle (length 30 mm, outer diameter 510 μm, inner diameter 250 μm) with a stainless steel rod (length 5 mm, outer diameter 250 μm) was used for the implantation of the dialysis probe. A dialysis probe was implanted into the right atrial myocardium near the junction of the superior vena cava and the right atrium. After implantation, the dialysis probe was perfused with Ringer's solution (in mmol/L: NaCl 147, KCl 4, $CaCl_2$ 3) containing a cholinesterase inhibitor eserine (100 μmol/L), at a speed of 2 μl/min using a microinjection pump (CMA/102, Carnegie Medicin, Sweden). Experimental protocols were started 120 min after implantation of the dialysis probe. The dead space between the dialysis membrane and the sample tube was taken into account at the beginning of each dialysate sampling. In protocols 1 and 2 as described below, 8 μl of phosphate buffer (pH 3.5) was added to each sample tube before dialysate sampling, and each dialysate sampling period was set at 20 min (1 sample volume=40 μl). Half of the dialysate sample was used for ACh and the other half for NE measurements. In protocol 3, 2 μl of phosphate buffer was added to each sample tube before dialysate sampling, and each dialysate sampling period was set at 5 min (1 sample volume=10 μl). In protocol 4, 4 μl of phosphate buffer was added to each sample tube before dialysate sampling, and each dialysate sampling period was set at 10 min (1 sample volume=20 μl). Dialysate NE and ACh concentrations were analyzed separately by high-performance liquid chromatography as described previously.[12,13]

Experimental Protocols

Protocol 1 (n=7) Baseline dialysate was sampled before the injection of medetomidine. Thereafter, a low dose (10 μg/kg) of medetomidine was injected intravenously via the femoral vein. After allowing 20 min for hemodynamic stabilization, dialysate was sampled for 20 min (40 μl). When the hemodynamics had recovered to the baseline level, a high dose (100 μg/kg) of medetomidine was injected intravenously and another 20-min dialysate sample was collected after hemodynamic stabilization. Finally, the vagal nerves were sectioned bilaterally at the neck and a dialysate sample was collected immediately after vagotomy. In 4 rabbits, an α_2-adrenergic antagonist, atipamezole (2.5 mg/kg), was intravenously administered before euthanasia and hemodynamic responses were recorded.

Protocol 2 (n=7) To prevent possible interference of medetomidine-induced hypotension with vagal nerve activity, intravenous infusion of an α_1-adrenergic agonist, phenylephrine, was started simultaneous to intravenous injection of medetomidine. Baseline dialysate sample was collected for 20 min before medetomidine injection. Simultaneous to intravenous injection of high-dose (100 μg/kg) medetomidine, intravenous infusion of phenylephrine was started (6.6±1.2 μg·kg^{-1}·min^{-1}) to maintain the mean blood pressure (BP) at baseline level. After hemodynamic stabilization, dialysate was sampled for 20 min. Finally, dialysate was again sampled immediately after bilateral cervical vagotomy.

Protocol 3 To investigate the effect of medetomidine on baroreflex-induced vagal ACh release, we varied the mean BP by changing the dose of intravenous phenylephrine in both the control (n=5) and medetomidine-treated (n=7) groups. In the control group, Ringer's solution was infused intravenously at 1.0 ml·kg^{-1}·h^{-1} throughout the experiment. In the medetomidine-treated group, medetomidine was initially injected intravenously at a dose of 60 μg/kg, and thereafter continuously infused at a dose of 60 μg·kg^{-1}·h^{-1} or a rate of 1.0 ml·kg^{-1}·h^{-1}. After baseline dialysate sampling, mean BP was increased in a stepwise manner by altering the dose of intravenous phenylephrine (maximal dose: 32.2±5.5 μg·kg^{-1}·min^{-1} in the control group and 18.6±2.1 μg·kg^{-1}·min^{-1} in the medetomidine-treated group). Dialysate samples were collected for 5 min at 4–7 different mean BP levels. Relations of log ACh concentrations vs. mean BP were plotted and regression lines for each animal were calculated.

Protocol 4 (n=5) We investigated the peripheral effects of medetomidine on heart rate and dialysate ACh concentration under electrical stimulation of the right cervical vagal nerve. Bilateral vagal nerves were exposed through a midline cervical incision and sectioned at the neck. A pair of bipolar stainless steel electrodes was attached to the efferent side of the

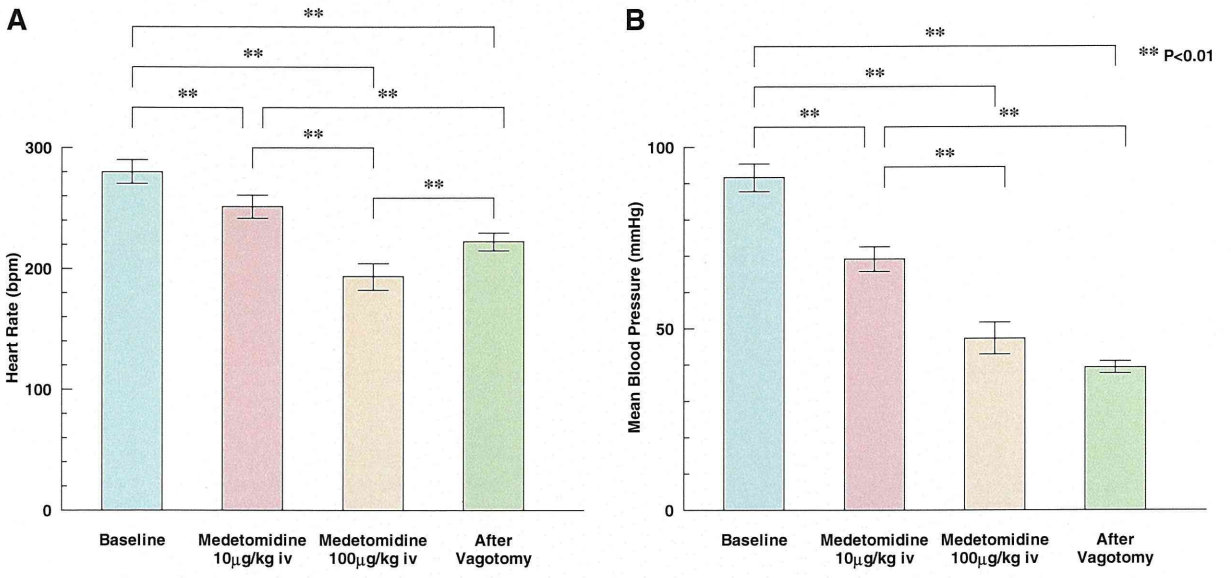

Figure 1. Intravenous administration of low and high doses of medetomidine decreased heart rate (**A**) and mean blood pressure (**B**). Medetomidine decreased heart rate in a dose-dependent manner. Vagotomy partially restored the decrease in heart rate but had no effect on mean blood pressure under administration of 100 μg/kg of medetomidine. **P<0.01.

right vagal nerve. The nerve and electrode were covered with warmed mineral oil for insulation. After the baseline dialysate sampling, the right efferent vagal nerve was stimulated at the frequency of 20 Hz by a digital stimulator (SEN-7203, Nihon Kohden, Japan). The pulse duration and amplitude of nerve stimulation were set at 1 ms and 10 V. Thereafter, a low dose (10 μg/kg) of medetomidine was injected intravenously via the femoral vein. After hemodynamic stabilization, dialysate was sampled for 10 min under the 20-Hz electrical stimulation of vagal nerve. Finally, a high dose (100 μg/kg) of medetomidine was injected intravenously and another 10-min dialysate sample was collected under the 20-Hz electrical stimulation.

Statistical Analysis

All data are presented as mean±standard error. Heart rate and mean BP were compared by 1-way repeated measures analysis of variance (ANOVA) followed by a Tukey's test.[14] Dialysate NE and ACh concentrations were also compared by 1-way repeated measures ANOVA followed by a Tukey's test. Comparisons of data between protocols 1 and 2 were conducted using unpaired t-test (Student's or Welch's t-test). In protocol 3, the average slopes and intercepts of the regression lines were compared using unpaired t-test. Differences were considered significant at P<0.05.

Results

Protocol 1

Intravenous injection of medetomidine significantly decreased heart rate (**Figure 1A**) and mean BP (**Figure 1B**) in a dose-dependent manner (280±10 beats/min and 92±4 mmHg, respectively, at baseline; 251±10 beats/min and 69±3 mmHg at 10 μg/kg; and 193±11 beats/min and 47±4 mmHg at 100 μg/kg, P<0.01 for all comparisons). Vagotomy increased heart rate to 222±7 beats/min but did not affect mean BP (**Figures 1A,B**).

Low-dose medetomidine significantly decreased dialysate NE concentration (**Figure 2A**) from 0.72±0.06 to 0.59±0.04 nmol/L (P<0.01) but did not affect dialysate ACh concentration (**Figure 2B**) compared with baseline. High-dose medetomidine also decreased dialysate NE concentration (to 0.52±0.05 nmol/L) similar to low-dose medetomidine (**Figure 2A**) and significantly increased dialysate ACh concentration from 7.2±1.3 nmol/L at baseline to 12.1±1.6 nmol/L (P<0.01, **Figure 2B**). Dialysate NE concentration was not changed by vagotomy, whereas dialysate ACh concentration recovered to the baseline level immediately after vagotomy (**Figures 2A,B**).

In 4 rabbits treated with atipamezole, heart rate and mean BP recovered to the baseline levels immediately after the injection (276±18 beats/min and 88±6 mmHg, respectively, at baseline; and 280±11 beats/min and 83±6 mmHg after the injection).

Protocol 2

Intravenous injection of high-dose medetomidine combined with phenylephrine decreased heart rate (**Figure 3A**) and the decrease was significantly greater than that observed in protocol 1 (140±9 vs. 193±11 beats/min, P<0.01), while mean BP was maintained at the same level as baseline (**Figure 3B**). Medetomidine combined with phenylephrine decreased dialysate NE concentration from 0.85±0.09 at baseline to 0.68±0.10 nmol/L (**Figure 4A**), and the decrease was not significantly different from that of medetomidine alone (protocol 1). However, medetomidine combined with phenylephrine increased dialysate ACh concentration (**Figure 4B**) to a significantly and markedly higher level than that observed in protocol 1 (26.8±5.4 vs. 12.1±1.6 nmol/L, P<0.05). Dialysate ACh concentration recovered to the baseline level immediately after vagotomy.

Protocol 3

The change in mean BP by phenylephrine administration affected dialysate ACh concentration only slightly in the control group (**Figure 5A**), whereas the elevation of mean BP